Search for suitable approximation methods for fullerene structure and relative stability studies: Case study with C_{50}

Wei Quan Tian[a)]
Department of Material Sciences, Faculty of Engineering Sciences, Kyushu University, 6-1 Kasugakoen, Kasuga, Fukuoka 816-8580, Japan

Ji-Kang Feng
State Key Laboratory of Theoretical and Computational Chemistry, Institute of Theoretical Chemistry, Jilin University, Changchun 130061, People's Republic of China and College of Chemistry, Jilin University, Changchun 130061, People's Republic of China

Yan Alexander Wang
Department of Chemistry, University of British Columbia, Vancouver, British Columbia V6T 1Z1, Canada

Yuriko Aoki
Department of Material Sciences, Faculty of Engineering Sciences, Kyushu University, 6-1 Kasugakoen, Kasuga, Fukuoka 816-8580, Japan and Group, PRESTO, Japan Science and Technology Agency (JST), Kawaguchi Center Building, Honcho 4-1-8, Kawaguchi, Saitama 332-0012, Japan

(Received 23 January 2006; accepted 13 July 2006; published online 5 September 2006)

Local density approximation (LDA), several popular general gradient approximation (GGA), hybrid module based density functional theoretical methods: SVWN, BLYP, PBE, HCTH, B3LYP, PBE1PBE, B1LYP, and BHandHLYP, and some nonstandard hybrid methods are applied in geometry prediction for C_{60} and C_{70}. HCTH with 3-21G basis set is found to be one of the best methods for fullerene structural prediction. In the predictions of relative stability of C_{50} isomers, PM3 is an efficient method in the first step for sorting out the most stable isomers. HCTH with 3-21G predicts very good geometries for C_{50}, similar to the performance of B3LYP/6−31G(d). The gap between the highest occupied molecular orbital and the lowest unoccupied molecular orbital from the predictions of all the density functional theory methods has the following descending order: E_{gap}(half-and-half hybrid) $>$ E_{gap}(B3LYP) $>$ E_{gap}(HCTH)(GGA) $>$ E_{gap}(SVWN)(LDA).
© *2006 American Institute of Physics*. [DOI: 10.1063/1.2335436]

I. INTRODUCTION

Since the discovery[1] of the first fullerene member, C_{60}, studies on fullerenes have grown rapidly into an exciting interdisciplinary field, attracting attentions from physics,[2] chemistry,[3] materials science,[4,5] and biology.[6,7] Detailed studies on the electronic structure of fullerenes[8,9] certainly help us to understand the physicochemical properties of fullerenes and to facilitate experimental identification of new fullerene compounds.[10–12] Efficient and reliable electronic structure methods are prerequisite for accurate predictions of the structures of fullerenes. Since the number of fullerene isomers increases drastically with the increases of the size of fullerene,[8] the most sophisticated and accurate theories (e.g., coupled cluster) are far beyond the affordability for the studies of fullerenes even with the rapid growth of computing resources. To search for suitable methods to study fullerenes, we perform benchmark calculations with some density functional theory (DFT) based methods with minimum and moderate basis sets on C_{60} and C_{70} with respect to available experimental data or other high-level theoretical calculations.

According to the isolated pentagon rule (IPR),[13] the IPR fullerene isomers are more stable than the non-IPR isomers of the same size. Thus far, IPR fullerene isomers with size up to C_{100} have been well studied.[14] The smallest IPR fullerene is C_{60} with I_h symmetry and the next one is C_{70} with D_{5h} symmetry. There is no IPR isomer from C_{62} to C_{68}. Because of the large number of isomers consisting of only hexagons and pentagons, a few studies have been carried out on fullerenes from C_{62} to C_{68} and from C_{52} to C_{58}. We perform extensive studies on the relative stability of C_{50} within DFT to search efficient and reliable methods for structural and relative stability characterizations particularly for fullerenes from C_{52} to C_{68}, ahead of their experimental identification.

As the fullerene size gets bigger, the factors controlling the relative stability of fullerene isomers, such as steric effect and π electron conjugation, change. Thus, theoretical methods suitable for small carbon clusters or small fullerenes may not be applicable to large fullerenes. There are several investigations to evaluate the methods used in fullerene characterization.[15] However, no study has focused on the accuracy of the prediction on the relative stability of the fullerene isomers of the same size and the geometric effect on the prediction of relative stability of fullerence isomers. Because of their similar sizes and the non-IPR nature of the fullerenes from C_{50} to C_{68} and the relatively small number of isomers of C_{50}, C_{50} is chosen as the first test system for the studies of fullerenes from C_{50} to C_{68}. Because C_{60} and C_{70}

[a)]Author to whom correspondence should be addressed. Fax: 81-92-583-8834. Electronic mail: wqtian@cube.kyushu-u.ac.jp

 © 2006 American Institute of Physics

Downloaded 08 Sep 2006 to 137.82.31.244. Redistribution subject to AIP license or copyright, see http://jcp.aip.org/jcp/copyright.jsp

are the two most abundant fullerenes whose experimental structures are readily available,[16–19] we thus use the experimental geometries of C_{60} and C_{70} to benchmark the performance of some DFT methods.

II. COMPUTATIONAL DETAILS

Because of the favorable computational scaling factor ($\propto N^3$, for the system size N) and predictive accuracy of the generalized gradient approximation (GGA) based DFT methods,[20–22] we concentrate our efforts on the most popular GGA based DFT methods: BLYP,[23,24] PBE,[25] and HCTH,[22] for geometry optimization. Though the higher formal scaling factor ($\propto N^4$, because of the exact exchange) makes the hybrid DFT methods unfavorable for large systems, the hybrid DFT methods are the proper choices for thermochemistry and geometry predictions.[21,26] We apply the hybrid DFT methods: B3LYP,[26] PBE1PBE,[27] B1LYP,[28] and BHandHLYP,[29] and some nonstandard hybrid methods with varied weights for the exact exchange and the GGA exchange in the geometry and relative energy predictions for C_{60} and C_{70}. In the nonstandard hybrid methods, three sets of modules are employed: BH$_x$LYP, BH$_x$B95, and PBEH$_x$PBE, where H$_x$ stands for the exact exchange with weight x ($1-x$ is the weight for the GGA exchange). The HCTH (HCTH-407) (Ref. 22) method was fitted with 407 sets of data including thermochemistry and geometry gradients and has comparable performance to B3LYP in thermochemistry and structure prediction.[22] Due to its efficiency, local density approximation (LDA), SVWN,[30,31] is also applied to C_{60}, C_{70}, and C_{50} for geometry optimization.

The geometries of the 271 isomers of C_{50} consisting of only pentagons and hexagons are optimized with the semiempirical PM3 (Ref. 32) method and further refined with SVWN with the STO-3G basis set. The geometries of the first 40 most stable isomers from single-point B3LYP/6-31G(d) calculations are further optimized with HCTH/3-21G and B3LYP/6-31G(d). HCTH/3-21G is chosen in geometry optimization for C_{50} due to its good performance in the geometry optimization for C_{60} and C_{70}. BHandHLYP, BHandHB95, and PBEHandHPBE, in which the half-and-half model was applied, and B3LYP with 6-31G(d) single-point energy calculations are carried out for the first 40 most stable isomers with the HCTH/3-21G geometries. Single-point energy calculations are further carried out with B3LYP/6-31G(d) based on the B3LYP/6-31G(d) geometries for the first 40 most stable C_{50} isomers. With the 6-311G(d) basis set, we refine the relative energies of the first three most stable C_{50} isomers and explore the convergence of relative energy with respect to the convergence of the density. GAUSSIAN 03 quantum chemical package[33] is employed for all these calculations.

Recent studies indicated that density functional tight binding method performs well in structure and relative energy characterizations of fullerenes without outperforming DFT methods.[34] We hence mainly focus on DFT and some semiempirical methods for fullerene studies in this study.

III. RESULTS AND DISCUSSIONS

A. Geometry predictions for C_{60} and C_{70}

As the molecular size of fullerene gets big, the balance between accuracy and efficiency becomes important in fullerene modeling. We apply four different basis sets, STO-3G, 3-21G, 6-31G, and 6-31G(d), in the geometry optimizations for C_{60} and C_{70}. The optimized bond distances are listed in Table I. The deviation (Δr) and the relative deviation ($\Delta\Delta r$) of the predicted bond distances from their experimental values are calculated through

$$\Delta r = \frac{\Sigma_i n_i |r_i^{\mathrm{expt}} - r_i|}{\Sigma_i n_i} \tag{1}$$

and

$$\Delta\Delta r = \frac{\Sigma_i n_i |r_i^{\mathrm{expt}-r_i}|/r_i^{\mathrm{expt}}}{\Sigma_i n_i}, \tag{2}$$

respectively, where n_i is the number of identical bond distance r_i and r_i^{exp} is the corresponding experimental bond distance.

The best prediction for bond distances of C_{60} and C_{70} is not from the biggest basis set used, 6-31G(d), but from 3-21G for those methods listed in Table I. The best performance of 3-21G with various DFT methods indicates that the good performance of 3-21G with DFT methods is general, although this is accredited to fortuitous error cancellation from exchange-correlation functional and basis set. Bond distances predicted with STO-3G have the largest error among the data collected. The improvement in geometry prediction from STO-3G to 3-21G is conspicuous and significant. Further addition of contracted functions from 3-21G to 6-31G does not necessarily improve the quality of geometry prediction. Similarly, inclusion of polarization functions from 6-31G to 6-31G(d) does not improve the accuracy much.

Methods converge with respect to basis set differently: geometry predictions with B3LYP, BLYP, PBE, and HCTH are drastically improved from STO-3G to split valence basis sets, while SVWN and PBE1PBE predict fairly good geometries for C_{60} and C_{70} even with STO-3G. In terms of computational efficiency and accuracy, 3-21G is the best basis set with present DFT methods to predict geometries of fullerenes. Among all the methods used, B3LYP/3-21G predicts the overall best geometries for C_{60} and C_{70}, followed by HCTH/3-21G and PBE1PBE/3-21G. The favorable computation scaling factor of the GGA ($\propto N^3$) over the hybrid method with the exact exchange ($\propto N^4$) makes HCTH/3-21G the best choice to predict geometries of fullerene. The average bond distance deviations for C_{70} and C_{60} within HCTH/3-21G are 0.012 and 0.002 Å, respectively. However, the maximum bond distance deviation from experiment for C_{70} predicted by HCTH/3-21G is large: 0.070 Å for the equatorial bond $r_{e\text{-}e}$.

SVWN, especially with STO-3G, performs surprisingly well on the bond distance prediction for C_{60} and C_{70}. SVWN/STO-3G predicts the second best geometry among

Downloaded 08 Sep 2006 to 137.82.31.244. Redistribution subject to AIP license or copyright, see http://jcp.aip.org/jcp/copyright.jsp

TABLE I. Bond distances (for each method, the four rows of bond distances in descending order are optimized with STO-3G, 3-21G, 6-31G, and 6-31G(d) basis sets, respectively) bond distance deviations (Δr), and relative bond distance deviations ($\Delta\Delta r$) from experiment and total energy variations (ΔE) for C_{60} and C_{70} calculated by various density functional theory based method. Δr and $\Delta\Delta r$ are defined in Eqs. (1) and (2), respectively. All energies are calculated with B3LYP/6-31G(d) for each optimized geometry and B3LYP/6-31G(d)//HCTH/3-21G energy is used as reference. Distance is in Å and energy is in kcal/mol. The density converges to 10^{-8} in the energy calculations.

	C_{70}											C_{60}				
Methods	$r_{a\text{-}a}$	$r_{a\text{-}b}$	$r_{b\text{-}c}$	$r_{b\text{-}c}$	$r_{c\text{-}d}$	$r_{d\text{-}d}$	$r_{d\text{-}e}$	$r_{e\text{-}e}$	Δr	$\Delta\Delta r$	ΔE	$r_{6\text{-}6}$	$r_{6\text{-}5}$	Δr	$\Delta\Delta r$	ΔE
	1.477	1.415	1.472	1.405	1.476	1.452	1.441	1.494	0.023	0.016	24.16	1.413	1.478	0.022	0.016	20.80
B3LYP	1.459	1.392	1.455	1.383	1.456	1.436	1.419	1.475	0.010	0.007	0.83	1.391	1.460	0.002	0.001	0.99
	1.459	1.399	1.454	1.390	1.456	1.439	1.424	1.477	0.012	0.008	0.93	1.398	1.460	0.006	0.005	1.03
	1.452	1.397	1.448	1.389	1.450	1.434	1.421	1.471	0.013	0.009	−0.26	1.395	1.454	0.003	0.002	−0.07
	1.489	1.431	1.484	1.423	1.485	1.469	1.455	1.506	0.035	0.024	62.76	1.429	1.490	0.037	0.026	54.22
BLYP	1.469	1.406	1.466	1.398	1.464	1.452	1.431	1.485	0.017	0.012	10.03	1.404	1.470	0.014	0.010	8.75
	1.469	1.412	1.465	1.405	1.464	1.454	1.436	1.487	0.019	0.013	13.53	1.411	1.470	0.018	0.013	12.05
	1.462	1.410	1.459	1.403	1.457	1.449	1.432	1.481	0.017	0.012	6.56	1.409	1.464	0.015	0.011	5.77
	1.478	1.423	1.474	1.415	1.474	1.460	1.446	1.494	0.026	0.018	33.61	1.422	1.479	0.029	0.020	29.05
PBE	1.464	1.403	1.460	1.395	1.459	1.447	1.427	1.478	0.015	0.010	4.52	1.402	1.465	0.011	0.008	3.92
	1.463	1.408	1.459	1.401	1.457	1.448	1.431	1.479	0.017	0.012	5.65	1.406	1.464	0.013	0.009	5.28
	1.456	1.406	1.452	1.399	1.451	1.443	1.427	1.473	0.016	0.011	1.67	1.405	1.457	0.010	0.007	1.55
	1.467	1.406	1.462	1.396	1.466	1.442	1.432	1.483	0.015	0.010	7.66	1.405	1.467	0.013	0.009	6.54
PBE1PBE	1.454	1.389	1.450	1.380	1.452	1.432	1.415	1.468	0.011	0.007	0.80	1.387	1.455	0.003	0.002	0.86
	1.453	1.395	1.448	1.386	1.450	1.433	1.419	1.470	0.012	0.009	−0.13	1.393	1.454	0.002	0.001	0.00
	1.446	1.392	1.442	1.384	1.444	1.428	1.416	1.464	0.015	0.010	1.36	1.391	1.448	0.002	0.002	1.33
	1.470	1.417	1.466	1.410	1.466	1.452	1.440	1.487	0.020	0.014	17.69	1.416	1.471	0.022	0.016	15.24
HCTH	1.455	1.395	1.451	1.388	1.450	1.437	1.419	1.468	0.012	0.008	0.00	1.394	1.455	0.002	0.001	0.00
	1.454	1.401	1.450	1.394	1.449	1.439	1.423	1.471	0.015	0.010	0.16	1.400	1.455	0.006	0.004	0.27
	1.446	1.398	1.443	1.392	1.442	1.433	1.420	1.465	0.017	0.012	0.65	1.397	1.448	0.006	0.004	0.75
	1.464	1.410	1.460	1.403	1.460	1.447	1.433	1.478	0.017	0.012	7.44	1.409	1.465	0.015	0.011	6.61
SVWN	1.449	1.390	1.445	1.383	1.444	1.433	1.414	1.461	0.014	0.009	1.45	1.389	1.450	0.003	0.002	1.11
	1.448	1.396	1.444	1.389	1.443	1.435	1.417	1.463	0.016	0.011	0.60	1.395	1.449	0.005	0.003	0.47
	1.441	1.394	1.438	1.387	1.437	1.429	1.414	1.457	0.017	0.012	4.03	1.392	1.442	0.005	0.003	3.53
B1LYP	1.452	1.396	1.448	1.387	1.449	1.433	1.420	1.471	0.013	0.009		1.394	1.453	0.003	0.002	
$BH_{30}LYP$[a]	1.449	1.393	1.446	1.384	1.448	1.430	1.418	1.469	0.013	0.009		1.408	1.474	0.018	0.013	
$BH_{35}LYP$[b]	1.448	1.390	1.444	1.381	1.447	1.427	1.415	1.467	0.013	0.009		1.404	1.472	0.014	0.010	
$BH_{40}LYP$[b]	1.446	1.388	1.442	1.378	1.446	1.425	1.413	1.466	0.013	0.009		1.400	1.470	0.011	0.008	
$BH_{45}LYP$	1.444	1.385	1.440	1.375	1.444	1.422	1.411	1.464	0.015	0.010		1.397	1.468	0.008	0.006	
BHandHLYP	1.442	1.383	1.438	1.373	1.443	1.419	1.409	1.463	0.016	0.011		1.394	1.466	0.006	0.004	
PM3	1.457	1.386	1.453	1.374	1.463	1.426	1.412	1.464	0.008	0.005		1.384	1.458	0.006	0.004	
Expt[b]	1.461	1.388	1.453	1.386	1.468	1.425	1.405	1.538				1.391	1.455			

[a]The subscript between "BH" and "LYP" is the weight of the exact exchange in the hybrid method; this notation applies to all nonstandard hybrid methods as explained in the text. The basis set employed is 6-31G(d).

[b]Experimental bond distances of C_{60} and C_{70} are from Refs. 16 and 17, respectively. The denotation for bond distances of C_{70} is from Ref. 17.

all the methods with STO-3G. Nonetheless, general application of SVWN/STO-3G in fullerene geometry optimization needs further verification. The predicted bond distances from STO-3G with other GGA and hybrid methods, except for PBE1PBE, have large deviations from experiment. The overall performance of SVWN on geometry prediction for C_{60} and C_{70} is slightly inferior (but comparable) to PBE1PBE and much superior to BLYP. In terms of computational efficiency and reliability (especially the former), SVWN/STO-3G (or better with 3-21G) should be the first choice for large fullerene modeling.

Amazingly, PM3 performs extremely well on the geometry prediction for C_{60} and C_{70} among all the methods employed: it has the smallest average bond distances deviation (only 0.008 Å) from experiment for C_{70},[35–37] and it does fairly well on geometry prediction for C_{60} (Refs. 35 and 36) (with the average bond distance deviation of 0.006 Å). The good performance of semiempirical methods, such as PM3, on fullerene structure prediction is not rare.[38,39] The equatorial bond distance deviation (0.074 Å) from experiments predicted by PM3 and other methods is large for C_{70}. However, one has to bear in mind that there is a large uncertainty in the gas-phase experiments on the equatorial bond distance of C_{70}.[17–19] All the predicted equatorial bond distances, on the other hand, agree very well with the x-ray observation.[19] Such large bond distance deviation in the prediction of all the methods on the equatorial bond of C_{70} is quite unusual. The

Downloaded 08 Sep 2006 to 137.82.31.244. Redistribution subject to AIP license or copyright, see http://jcp.aip.org/jcp/copyright.jsp

reliability of all the methods used for fullerene structure prediction needs further calibrations once more refined experimental data of fullerenes are available.

The role of the exact exchange in geometry prediction for C_{60} and C_{70} can be seen from the improvement in the optimized geometries from BLYP to B3LYP and from PBE to PBE1PBE. The most significant improvement by the exact exchange occurs with STO-3G. Augmentation of the basis set from STO-3G to 3-21G narrows the performance gap between the GGA and the hybrid method for geometry prediction. The variation of the weight of the exact exchange in the hybrid method affects geometry prediction as well. In the BH$_x$LYP module for the geometry optimizations of C_{60} and C_{70}, the weight of the exact exchange x is increased from 0.25 (in B1LYP) to 0.50 (in BHandHLYP) by a step of 0.05, resulting in BH$_{30}$LYP (x=0.30), BH$_{35}$LYP (x=0.35), BH$_{40}$LYP (x=0.40), and BH$_{45}$LYP (x=0.45). Among the BLYP-based hybrid methods, B1LYP and B3LYP with 6-31G(d) perform the best on the geometry predictions for C_{60} and C_{70}. As the weight of the exact exchange increases, the performance of the hybrid methods on the geometry prediction of C_{70} deteriorates.

The bond distance and relative bond distance deviations are the average and overall geometric indices for the performance of the applied methods in geometry prediction. Geometry deviation from experiment cannot be completely reflected through such indices since they do not reveal the direction of bond distance deviation. The predicted individual bond distances can serve as supplementary indices for this purpose. From the data shown in Table I, all the DFT methods overall underestimate the bond distances for C_{60} and C_{70}, and the most conspicuous underestimation is on the equatorial bond distance $r_{e\text{-}e}$ (1.538 Å) (Ref. 17) in C_{70}. The largest deviation from experiment, 0.081 Å, of this bond distance is from SVWN/6-31G(d). Another complementary index for geometry deviation is energy change upon geometric variation. The relative energy, reflecting the geometric variation of the optimized geometry from that of HCTH/3-21G, is crucial in searching for the most stable isomers of a particular fullerene if many isomers have similar energies. We carry out single-point calculations with B3LYP/6-31G(d) on the optimized geometries of C_{60} and C_{70} and use the B3LYP/6-31G(d)//HCTH/3-21G results as the reference. According to the relative energy prediction and the average bond distance deviation from different methods and basis sets (shown in Table I), PBE1PBE and SVWN have the best geometry prediction capacity and the smallest basis set dependency.

B. Geometries and relative stability of C_{50}

C_{50} has 271 isomers consisting of only hexagons and pentagons: 195 isomers with C_1 symmetry, 37 isomers with C_2 symmetry, 25 isomers with C_s symmetry, 2 isomers with C_3 symmetry, 6 isomers with C_{2v} symmetry, 2 isomers with D_3 symmetry, 1 isomer with C_{3v} symmetry, 1 isomer with D_{3h} symmetry, and 2 isomers with D_{5h} symmetry. The total number of C_{50} isomers is large enough for statistical treatment and small enough for accurate and affordable methods. The structures and relative stabilities of C_{50} isomers were studied extensively with semiempirical methods and several most stable isomers were further studied with B3LYP/6-31G(d).[40] Two isomers with D_{5h} and D_3 symmetries are the most stable isomers of C_{50}: the D_3 isomer is 2.0 kcal/mol more stable than the D_{5h} isomer according to the B3LYP/6-31G(d) prediction.[40] Sphericity was found to be the controlling factor on the relative stability of C_{50} isomers.[41] It was found that the switch of the highest occupied molecular orbital (HOMO) and the lowest unoccupied molecular orbital (LUMO) of the electronic wave function of C_{50} results in two electronic states with very close total energies.[42]

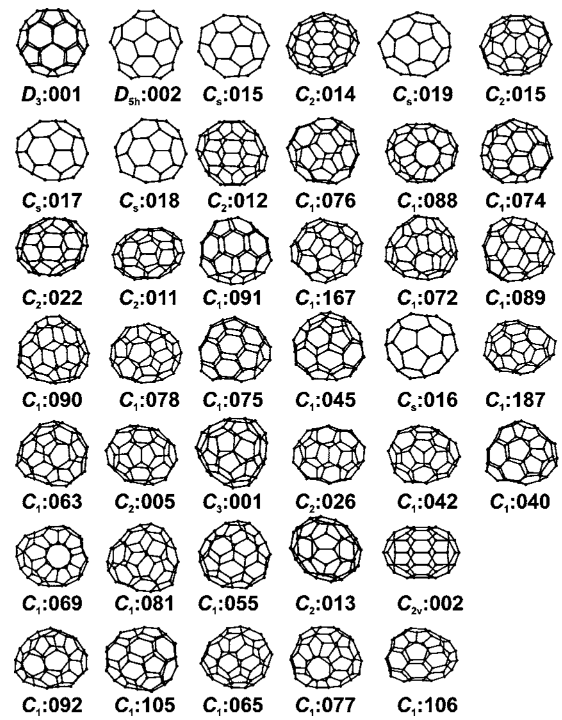

FIG. 1. Structures of the first 40 most stable C_{50} isomers.

In the present work, we focus on the relative stability and the HOMO-LUMO gap of C_{50} isomers. The C_{50} structures are constructed with the FULLGEN code.[43] The first 40 most stable isomers in energetic order are shown in Fig. 1. The numeric indices of the C_{50} isomers follow their order of appearance in the output file within each distinct symmetry.

1. The relative stability and the HOMO-LUMO gaps of C_{50}

The relative energies of all C_{50} isomers from SVWN/STO-3G//SVWN/STO-3G, B3LYP/6-31G(d)//SVWN/STO-3G, and B3LYP/6-31G(d)//PM3 are plotted against the relative energies from PM3//PM3 in Fig. 2(a). The relative energies from different methods correlate very well. Accredited to its computational efficiency, the good correlation of relative energies from different methods with that of PM3 assures PM3 as the method of choice for preliminary geometry optimization to sort out the most stable fullerene isomers. Qualitatively, the geometric effect on the relative energy prediction is negligible, as verified by the correlation of the B3LYP/6-31G(d)//PM3 relative energies

Downloaded 08 Sep 2006 to 137.82.31.244. Redistribution subject to AIP license or copyright, see http://jcp.aip.org/jcp/copyright.jsp

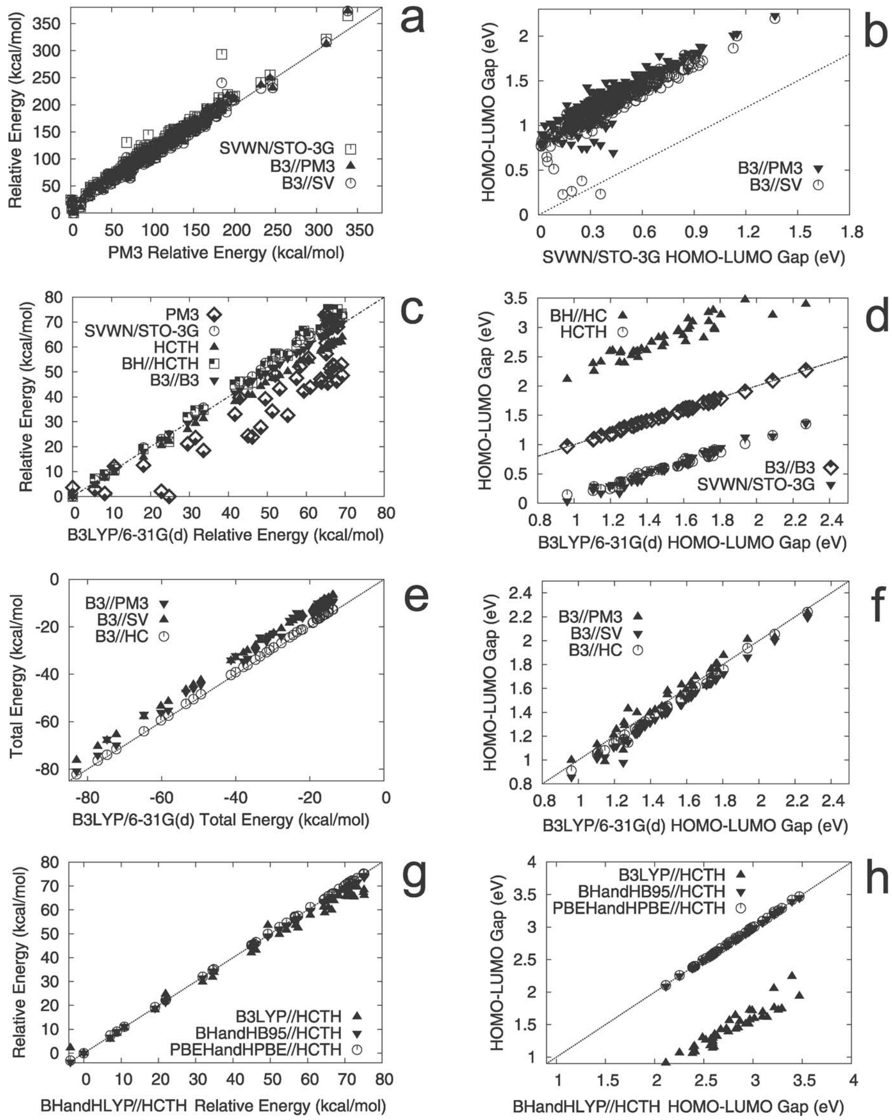

FIG. 2. Relative energies and the energy gap between the highest occupied molecular orbital (HOMO) and the lowest unoccupied molecular orbital (LUMO) of C_{50} isomers at different levels of theory. B3//PM3, B3//SV, BH//HCTH, and B3//B3 stand for B3LYP/6-31G(d)//PM3, B3LYP/6-31G(d)//SVWN/STO-3G, BHandHLYP/6-31G(d)//HCTH/3-21G, and B3LYP/6-311G(d)//B3LYP/6-31G(d), respectively. (a) Relative energies of the 271 C_{50} isomers at different levels of theory. PM3 relative energies are predicted from the PM3 geometries. (b) The HOMO-LUMO gap of the 271 C_{50} isomers predicted by SVWN/STO-3G, B3LYP/6-31G(d) based on the PM3 and SVWN/STO-3G geometries. The SVWN/STO-3G HOMO-LUMO gaps are predicted from the SVWN/STO-3G geometries. (c) The relative energies of the first 40 most stable C_{50} isomers at different levels of theory. B3LYP/6-31G(d) relative energies are predicted from the B3LYP/6-31G(d) geometries. (d) The HOMO-LUMO gap of the 40 most stable C_{50} isomers at different levels of theory. B3LYP/6-31G(d) HOMO-LUMO gaps are predicted from the B3LYP/6-31G(d) geometries. (e) The total energies of the first 40 most stable C_{50} isomers predicted by B3LYP/6-31G(d) based on geometries from PM3, SVWN/STO-3G, and HCTH/3-21G. The total energy of each isomer is subtracted by −1904.800 000 a.u. B3LYP/6-31G(d) relative energies are predicted from the B3LYP/6-31G(d) geometries. (f) The HOMO-LUMO gap of the 40 most stable C_{50} isomers at different levels of theory based on geometries from PM3, SVWN/STO-3G, and HCTH/3-21G. B3LYP/6-31G(d) HOMO-LUMO gaps are predicted from the B3LYP/6-31G(d) geometries. (g) The relative energies of the first 40 most stable C_{50} isomers predicted by the half-and-half hybrid DFT methods with different exchange-correlation functionals based on the HCTH/3-21G optimized geometries. The 6-31G(d) basis set is employed for the calculations. (h) The HOMO-LUMO gap of the 40 most stable C_{50} isomers predicted by the half-and-half hybrid DFT methods with different exchange-correlation functionals based on the HCTH/3-21G optimized geometries. The 6-31G(d) basis set is employed for the calculations.

with the B3LYP/6-31G(d)//SVWN/STO-3G ones. An exception is the relative energy for the C_{2v}:001 isomer: SVWN/STO-3G predicts this isomer to have a much higher relative energy (about 50 kcal/mol) than the other methods do, which can be a deficiency in SVWN/STO-3G. The overall HOMO-LUMO gap predicted by SVWN/STO-3G is about 0.8 eV smaller than that from B3LYP/6-31G(d) with either PM3 or SVWN/STO-3G geometry. The sensitivity of the HOMO-LUMO gap to fullerene geometry, especially for fullerenes with small HOMO-LUMO gaps, is stronger than that of relative energy to geometry [as shown in Fig. 2(b): B3LYP/6-31G(d)//PM3 versus B3LYP/6-31G(d)//SVWN/STO-3G] for the isomers with small HOMO-LUMO gaps. For some C_{50} isomers with small HOMO-LUMO gaps, the gap based on the PM3 geometry is larger than that based on the SVWN/STO-3G geometry in the single-point B3LYP/6-31G(d) calculations. This variation in the HOMO-LUMO gap due to geometry change gets smaller as the HOMO-LUMO gap widens.

The first 40 most stable C_{50} isomers predicted from

Downloaded 08 Sep 2006 to 137.82.31.244. Redistribution subject to AIP license or copyright, see http://jcp.aip.org/jcp/copyright.jsp

TABLE II. Averaged and maximal bond distance deviations and their root mean squared deviations ($\Delta\Delta R$) (in Å) of the first 40 most stable C_{50} isomers, calculated at PM3, SVWN/STO-3G, and HCTH/3-21G with respect to the B3LYP/6-31G(d) geometries. $\Delta\Delta R$ is defined in Eq. (3). M refers to maximal bond distance deviation from the B3LYP/6-31G(d) optimized geometry.

	PM3	PM3^M	SVWN	SVWN^M	HCTH	HCTH^M
Averaged	0.012	0.040	0.013	0.021	0.003	0.012
$\Delta\Delta R$	0.0005	0.0024	0.0000	0.0004	0.0001	0.0005

B3LYP/6-31G(d)//SVWN/STO-3G are optimized at the HCTH/3-21G level of theory, followed by single-point BHandHLYP, BHandHB95, PBEHandHPBE, and B3LYP calculations with 6-31G(d), and further refined with B3LYP/6-31G(d) based on the B3LYP/6-31G(d) geometries.[44] Due to the good performance of B3LYP/6-31G(d) on C_{60}, C_{70}, and fullerene related polyarenes,[45] the geometries and the relative energies of these isomers predicted by B3LYP/6-31G(d) are employed as reference. PM3 predicts smaller relative energies for these C_{50} isomers, i.e., more difficult to sort out the most stable isomers. PM3 predicts benzenelike D_{5h}:002 as the most stable C_{50} isomer, followed by C_s:017, C_2:015, quinoidlike D_{5h}:002, and D_3:001, and the benzenelike D_{5h}:002 to have much lower energy than the second most stable one (C_s:017). The most stable isomer predicted by DFT (except for the half-and-half hybrid DFT methods), on the other hand, is D_3:001, followed by D_{5h}:002, C_s:015 and C_2:014. The discrepancy between the relative energies predicted by PM3 and DFT is apparent for the first several most stable C_{50} isomers [see Fig. 2(c)], and such discrepancy advises caution in interpreting the PM3 relative energies. Thus, semiempirical method, such as PM3, is not suitable in searching for the most stable isomer for fullerenes.

The relative energies predicted by DFT methods correlate well with one another; even SVWN with minimum basis set is good enough for qualitative relative stability prediction for fullerenes. For small fullerenes (smaller than C_{70}), the methods employed in the present study are applicable because the relative energies among isomers are large. However, caution is advised in relative stability prediction for large fullerenes (bigger than C_{100}), since as the fullerene size gets larger, the energy difference among isomers gets smaller and the interplay among the relative stability, π electron conjugation, and performance of methods becomes very delicate.

2. Geometries of C_{50}

The overall average and maximal bond distance root mean squared (rms) deviations of the first 40 most stable isomers, calculated through

$$\Delta\Delta R = \frac{\sqrt{\Sigma_i \left| |\Delta r_i| - \overline{\Delta r} \right|^2}}{n}, \tag{3}$$

are listed in Table II.[44] $|\Delta r_i|$ is the average (maximal) bond distance deviation of isomers i, $\overline{\Delta r}$ is the overall average (maximal) bond distance deviation of the optimized geometries of each method from those B3LYP/6-31G(d) ones for the first 40 most stable C_{50} isomers, and n is the total number of conformations.

SVWN/STO-3G has the largest average bond distance deviation, which is 0.001 larger than that from PM3. HCTH/3-21G has the smallest deviation from the B3LYP/6-31G(d) geometry with the average bond distance deviation of 0.003 Å and the average maximal deviation of 0.012 Å. Thus, bond distances from HCTCH/3-21G are very close to those from B3LYP/6-31G(d). A close inspection of the maximum and rms deviations reveals that the PM3 has the largest bond distance deviation (0.075 Å). The PM3 bond distances fluctuate around the B3LYP/6-31G(d) ones from both directions (shorter and longer), SVWN/STO-3G systematically predicts longer bond distances for C_{50} than B3LYP/6-31G(d) does, and the HCTH/3-21G bond distances slightly fluctuate around the B3LYP/6-31G(d) ones.[44] Clearly, the geometry predicted by HCTH/3-21G is of the best quality and compares very well with the B3LYP/6-31G(d) predictions. Based on the predictions of the geometries of C_{60}, C_{70}, and C_{50}, the good performance of HCTH is not fortuitous.[22]

3. The HOMO-LUMO gap

The HOMO-LUMO gap has practical effect on the application of a method in molecular modeling: small (close to zero) HOMO-LUMO gap affects the convergence of electronic structure calculations through introducing higher electronic states, resulting in multiconfiguration character.

Among all the applied DFT methods, BHandHLYP/6-31G(d) predicts the largest HOMO-LUMO gap, followed by B3LYP/6-31G(d). Also, HCTH/3-21G has a similar gap to that from SVWN/STO-3G. As shown in Fig. 2(d), B3LYP/6-31G(d) predicts bigger gap (ca. 0.8 eV) than HCTH/3-21G and SVWN/STO-3G do, and BHandHLYP/6-31G(d) predicts bigger gap (ca. 1.1 eV) than B3LYP/6-31G(d) does. Clearly, the inclusion of the exact exchange increases the HOMO-LUMO gap. It is also true that the HOMO-LUMO gap does not necessarily correlate with the relative stability of fullerene isomers.[44] For the HOMO-LUMO gaps of some other π systems, the performance of DFT methods including LDA, GGA, and hybrid methods has been analyzed as well.[46] The effect of basis set, however, is not included in the present study for the HOMO-LUMO gap.

4. Correlation of geometry with the relative stability and the HOMO-LUMO gap

The effect of geometry on relative energies can be seen from the relative energies and the total energies predicted by

Downloaded 08 Sep 2006 to 137.82.31.244. Redistribution subject to AIP license or copyright, see http://jcp.aip.org/jcp/copyright.jsp

B3LYP/6-31G(d)//PM3, B3LYP/6-31G(d)//SVWN/STO-3G, and B3LYP/6-31G(d)//HCTH/3-21G for the first 40 most stable C_{50} isomers [shown in Fig. 2(e)]. The order of the relative stability of the first 40 C_{50} isomers predicted by these three methods is the same. The total energies and the HOMO-LUMO gaps predicted by these three methods are plotted in Figs. 2(e) and 2(f), respectively. The total energies of C_{50} isomers from B3LYP/6-31G(d)//PM3, B3LYP/6-31G(d)//SVWN/STO-3G, and B3LYP/6-31G(d)//HCTH/3-21G, especially the last one, correlate very well with those based on the B3LYP/6-31G(d) geometries, as indicated in Fig. 2(e). Both B3LYP/6-31G(d)//PM3 and B3LYP/6-31G(d)//SVWN/STO-3G predict higher energies for C_{50} isomers than B3LYP/6-31G(d)//HCTH/3-21G does. In other words, with respect to the geometry predicted by B3LYP/6-31G(d), HCTH/3-21G predicts better geometry for C_{50} than PM3 and SVWN/STO-3G do. To check the overall deviation of geometry predicted by different methods, we calculate the average total energy difference (ΔE^t) and average HOMO-LUMO gap difference (ΔE_{gap}) of C_{50} isomers from reference values obtained with the B3LYP/6-31G(d) geometry through the following equation:

$$\Delta E^t = \frac{\sum_i |E_i^r - E_i^t|}{n}, \tag{4}$$

where E_i^r is the reference total energy of the ith isomer, E_i^t is the total energy of the ith isomer, and n is the total number of isomers studied. ΔE_{gap} is calculated similarly after replacing the total energy by the HOMO-LUMO gap. The total energy and the HOMO-LUMO gap calculated at the B3LYP/6-31G(d) level for each isomer are used as the reference in Eq. (4). The average total energy differences (ΔE^t) of B3LYP/6-31G(d)//PM3, B3LYP/6-31G(d)//SVWN/STO-3G, and B3LYP/6-31G(d)//HCTH/3-21G are 5.57, 7.03, and 1.00 kcal/mol, respectively. Thus, HCTH/3-21G predicts closer geometry of C_{50} to the B3LYP/6-31G(d) geometry than the other two methods do. Based on this particular criterion, it seems that PM3 predicts geometry closer to that of B3LYP/6-31G(d) than SVWN/STO-3G does. However, the rms deviation from the average bond distance ($\Delta\Delta R$) reveals that SVWN/STO-3G systematically predicts better geometry; thus SVWN/STO-3G is more suitable for high-quality prediction of relative stability. The largest and smallest energy deviations of B3LYP/6-31G(d)//PM3 from those of B3LYP/6-31G(d)//B3LYP/6-31G(d) are 9.61 (for C_1:0.63) and 2.40 kcal/mol (for D_3:001), respectively. The corresponding values for B3LYP/6-31G(d)//SVWN/STO-3G and B3LYP/6-31G(d)//HCTH/3-21G are 7.84 (the largest, for C_1:092) and 6.49 kcal/mol (the smallest, for D_{5h}:002 benzenelike), and 1.40 (the largest, for C_3:001) and 0.53 kcal/mol (the smallest, for D_{5h}:002 benzenelike), respectively.

Following Eq. (4), ΔE_{gap} of B3LYP/6-31G(d)//PM3 is 0.01 eV larger than the one predicted by B3LYP/6-31G(d)//B3LYP/6-31G(d), while ΔE_{gap}'s of B3LYP/6-31G(d)//SVWN/STO-3G and B3LYP/6-31G(d)//HCTH/3-21G are 0.08 and 0.01 eV smaller than that of B3LYP/6-31G(d)//B3LYP/6-31G(d), respectively. The rms deviation from the average value [0.02 eV for B3LYP/6-31G(d)//PM3, 0.01 eV for B3LYP/6-31G(d)//SVWN/STO-3G, and 0.01 eV for B3LYP/6-31G(d)//HCTH/3-21G] indicates that B3LYP/6-31G(d)//HCTH/3-21G has the best performance compared with B3LYP/6-31G(d)//B3LYP/6-31G(d). Figure 2(f) further shows that B3LYP/6-31G(d)//PM3 predicts larger HOMO-LUMO gap and B3LYP/6-31G(d)//SVWN/STO-3G predicts smaller HOMO-LUMO gap than B3LYP/6-31G(d)//B3LYP/6-31G(d) does, while B3LYP/6-31G(d)//HCTH/3-21G predicts (smaller) HOMO-LUMO gap closest to those from B3LYP/6-31G(d)//B3LYP/6-31G(d). This further corroborates the good performance of HCTH/3-21G, similar to that of B3LYP/6-31G(d), in the geometry optimization of C_{50}.

Now, we further benchmark the relative stability of C_{50} isomers predicted by different methods based on the same geometry. The geometries of the first 40 most stable C_{50} isomers predicted by HCTH/3-21G are employed as the reference geometries. The half-and-half hybrid DFT methods (BHandHLYP, BHandHB95, and PBEHandHPBE) and B3LYP, with 6-31G(d) basis set, are employed for this investigation. Due to the similarity in the geometries of HCTH/3-21G and B3LYP/6-31G(d), the conclusion drawn based on the HCTH/3-21G geometry should not change if the B3LYP/6-31G(d) geometry is used instead. The relative energies of the C_{50} isomers with respect to the $C_{50}(D_3\!:\!001)$ isomer and their HOMO-LUMO gaps are plotted in Figs. 2(g) and 2(h), respectively. The three half-and-half hybrid DFT methods predict similar relative stability for C_{50} isomers and correlate very well with one another. All the half-and-half hybrid DFT methods predict the $C_{50}(D_{5h}\!:\!002)$ benzenelike tautomer to be most stable. On the other hand, B3LYP predicts $C_{50}(D_3\!:\!001)$ as the most stable isomer, though the energy difference between the structures of $C_{50}(D_{5h}\!:\!002)$ and $C_{50}(D_3\!:\!001)$ is very small. B3LYP correlates well with the half-and-half hybrid DFT methods for the remaining C_{50} isomers, but small fluctuation in the relative energies predicted by B3LYP from those of the half-and-half hybrid DFT methods becomes obvious when relative energy becomes large, from 20 to 80 kcal/mol [see Fig. 2(g)]. The HOMO-LUMO gaps predicted by the three half-and-half hybrid DFT methods are very close to one another [see Fig. 2(h)], while B3LYP/6-31G(d) predicts smaller HOMO-LUMO gap than the half-and-half hybrid DFT methods do. From this result, we can infer that the weight of the exact exchange has a more important role in the prediction of the HOMO-LUMO gap. The more the exact exchange is included in the hybrid DFT methods, the larger the HOMO-LUMO gap will be predicted. A closer inspection of the HOMO and the LUMO energies of the C_{50} isomers from these methods indicates that the exact exchange stabilizes the HOMO while destabilizes the LUMO, thus widening the HOMO-LUMO gap.

5. Refinement of the relative stability

The relative stability of the first 40 most stable C_{50} isomers predicted by all the methods essentially indicates that

Downloaded 08 Sep 2006 to 137.82.31.244. Redistribution subject to AIP license or copyright, see http://jcp.aip.org/jcp/copyright.jsp

TABLE III. Total energies (in a.u.) and relative stability (in kcal/mol) of the first three most stable C_{50} isomers from B3LYP/6-31G(d) single-point calculations with different convergence criteria for the root mean squared error in the density.

	B3LYP/6-31G(d)				HCTH/3-21G geometry			
Conver	D_3	D_{5h}[a]	D_{5h}[b]	ΔE[c]	D_3	D_{5h}[a]	D_{5h}[b]	ΔE
10^{-4}	−1904.933 310	−1904.936 708	−1904.929 264	−2.13(−2.54)	−1904.950 735	−1904.927 829	−1904.928 326[d]	14.37(14.06)
10^{-5}	−1904.932 210	−1904.923 124	−1904.928 427	5.70(2.37)	−1904.931 024	−1904.921 736	−1904.927 544	5.83(2.18)
10^{-6}	−1904.932 210	−1904.923 124	−1904.928 427	5.70(2.37)	−1904.931 024	−1904.921 736	−1904.927 544	5.83(2.18)
10^{-7}	−1904.932 210	−1904.923 124	−1904.928 427	5.70(2.37)	−1904.931 024	−1904.921 736	−1904.927 544	5.83(2.18)
10^{-8}	−1904.932 210	−1904.923 124	−1904.928 427	5.70(2.37)	−1904.931 024	−1904.921 736	−1904.927 544	5.83(2.18)

[a]The HOMO is A_1'.
[b]The HOMO is A_2'.
[c]The number in parentheses is the energy difference between $C_{50}(D_{5h}$:002[b]) and $C_{50}(D_3$:001).
[d]The first single-point calculation yields the total energy as −1904.905 528 a.u; with the first converged wave function, and the second single-point calculation with the same convergence criterion yields the total energy as −1904.928 326 a.u..

D_3:001 is the most stable isomer. However, the single-point half-and-half hybrid DFT calculations predict $C_{50}(D_{5h}$:002) benzenelike tautomer to be the most stable one. In a default single-point calculation using GAUSSIAN 03 package,[33] the rms error in density is only required to converge to 10^{-4}, which has lower convergence requirement than that during geometry optimization and might bring some numerical uncertainty in the relative energy prediction. With this default convergence criterion and based on the HCTH/3-21G geometry, the single-point BHandHB95/6-31G(d) calculations predict that $C_{50}(D_{5h}$:002) quinoidlike tautomer is 1.58 kcal/mol more stable than $C_{50}(D_3$:001), whereas B3LYP/6-31G(d) predicts $C_{50}(D_3$:001) to be 14.37 kcal/mol more stable than $C_{50}(D_3$:001). The relative energy changes drastically for the three structures listed in Table III, when the convergence criterion of the rms error in density is tighten from 10^{-4} to 10^{-5}. With the 10^{-4} convergence, the total energy changes much with different initial guesses for wave functions,[44] but converges to its stable value with the tighter 10^{-5} convergence. On the other hand, the HOMO-LUMO gap is not very sensitive to the convergence of the density. For reliable relative energy prediction, the default rms error in density convergence (10^{-4}) in single-point calculation is not enough and must be tightened at least to 10^{-5}.

We further perform single-point calculations on the first three most stable C_{50} isomers, D_3:001, D_{5h}:002, and C_s:015, using B3LYP and MP2 with the 6-311G(d) basis set. The relative energies of the three C_{50} isomers from these predictions are listed in Table IV, where the influence of the density convergence to the relative stability of fullerene isomers is again revealed. The relative stability of these four structures predicted by DFT with 6-311G(d) is similar to that by the same methods with 6-31G(d). The half-and-half hybrid DFT methods predict $C_{50}(D_{5h}$:002) benzenelike tautomer to be the most stable structure, while B3LYP predicts $C_{50}(D_3$:001) as the most stable one. MP2/6-31G(d), with both the HCTH/3-21G and B3LYP/6-31G(d) geometries, also predicts that $C_{50}(D_3$:001) is the most stable isomer and the two tautomers of $C_{50}(D_{5h}$:002) are at least 10 kcal/mol less stable. $C_{50}(C_s$:015) is the fourth most stable structure within DFT, but it is the second most stable structure within MP2/6-31G(d). Such discrepancy between DFT methods and MP2 in the prediction of relative energy is quite common.[47,48]

6. Quality of the relative stability and the HOMO-LUMO gap

The quality of the relative energies and the HOMO-LUMO gaps of C_{50} isomers predicted by each method can be measured by the average HOMO-LUMO gap difference ΔE_{gap} and the average relative energy difference ($\Delta\Delta E$) of all the methods employed,

$$\Delta\Delta E^t = \frac{\Sigma_i |\Delta E_i^r - \Delta E_i^t|}{n}, \tag{5}$$

where ΔE_i^r is the relative energy of the ith isomer with respect to the most stable isomer at the reference level of

TABLE IV. Relative energies (in kcal/mol) of the first three most stable C_{50} isomers predicted by BHandHLYP, B3LYP, BHandHB95, PBEHandHPBE, and MP2 with 6-3111G(d) based on the HCTH/3-21G geometry and by B3LYP and MP2 with 6-311G(d) based on the B3LYP/6-31G(d) geometry. The number in parentheses are the relative energies from single-point calculations with density convergence set to 10^{-4}. All the other relative energies have density convergence of 10^{-8}.

Isomers	BHandHLYP	BHandHB95	PBEHandHPBE	B3LYP	MP2	B3LYP[a]	MP2[b]
D_3:001	0.00	0.00	0.00	0.00	0.00	0.00	0.00
D_{5h}:002[b]	6.63(4.45)	6.37(10.15)	7.04(7.24)	5.41(3.74)	10.02	5.24	11.87
D_{5h}:002[c]	−2.52(−2.49)	−2.61(4.59)	−2.02(−1.33)	3.09(0.23)	19.23	3.29	19.12
C_s:015	8.80(9.51)	9.01(8.90)	8.97(9.99)	8.21(2.48)	9.38	8.15	9.32

[a]Based on the B3LYP/6-31G(d) geometry.
[b]The HOMO is A_1'.
[c]The HOMO is A_2'.

Downloaded 08 Sep 2006 to 137.82.31.244. Redistribution subject to AIP license or copyright, see http://jcp.aip.org/jcp/copyright.jsp

TABLE V. The average relative energy difference ($\Delta\Delta E$), defined in Eq. (4), of C_{50} isomers between the relative energy predicted by each method and the PM3 relative energy and the average HOMO-LUMO gap difference ΔE_{gap} defined in Eq. (4), of C_{50} isomers between the HOMO-LUMO gap predicted by each method and the SVWN/STO-3G HOMO-LUMO gap. The numbers in parentheses are relative energies calculated with density convergence set to 10^{-4}, and the other numbers are calculated with density convergence set to 10^{-8}.

	$\Delta\Delta E$ (kcal/mol)		ΔE_{gap} (eV)	
Method	All isomers	First 40 most stable isomers	All isomers	First 40 most stable isomers
PM3	0.00	0.00		
SVWN/STO-3G	17.08	14.72	0.00	0.000
B3LYP/6-31G(d)//PM3	(14.98)	15.44 (15.25)	0.883	0.898
B3LYP/6-31G(d)//SVWN/STO-3G	(12.10)	12.52 (12.96)	0.784	0.810
HCTH		9.17		0.049
B3LYP/6-31G(d)//HCTH/3-21G		12.60 (23.85)		0.854
BHandHLYP/6-31G(d)//HCTH/3-21G		14.77		2.192
BHandHB95/6-31G(d)//HCTH/3-21G		14.11 (14.09)		2.174
PBEHandHPBE/6-31G(d)//HCTH/3-21G		14.99 (15.95)		2.190
B3LYP/6-31G(d)		12.25		0.891
B3LYP/6-311G(d)//B3LYP/6-31G(d)		12.48		0.899

theory, ΔE_i^t is the relative energy of the ith isomer with respect to the most stable isomer from the method t, and n is the total number of isomers. The PM3 relative energy and the SVWN/STO-3G HOMO-LUMO gap are chosen as reference. All the average relative energy differences ($\Delta\Delta E$) and the average HOMO-LUMO gap differences (ΔE_{gap}) are listed in Table V. The geometric effect on the single-point calculations is indicated by the variation (2.92 kcal/mol) in the B3LYP/6-31G(d)//PM3 and B3LYP/6-31G(d)//SVWN/STO-3G average relative energy differences. The small relative energy difference among B3LYP/6-31G(d)//SVWN/STO-3G, B3LYP/6-31G(d)//HCTH/3-21G, and B3LYP/6-31G(d)//B3LYP/6-31G(d) indicates the similarity in the geometries predicted by these methods. Roughly speaking, all the DFT methods predict similar relative energies. The influence of the density convergence to the prediction of the relative energy is again revealed by the relative energies with the rms error in density converged to 10^{-5} and 10^{-4}. Overall, the sensitivity of the HOMO-LUMO gap to geometry is less strong than that of the relative energy, as manifested by the differences in the HOMO-LUMO gaps predicted by B3LYP/6-31G(d)//PM3, B3LYP/6-31G(d)//SVWN/STO-3G, B3LYP/6-31G(d)//HCTH/3-21G, and B3LYP/6-31G(d)//B3LYP/6-31G(d). However, the sensitivity of the HOMO-LUMO gap to method employed is quite clear. The three half-and-half hybrid DFT methods predict the largest HOMO-LUMO gaps, which are close to one another. According to Figs. 2(b), 2(d), 2(f), and 2(h), the HOMO-LUMO gaps predicted by DFT methods have this descending order: E_{gap}(half-and-half hybrid) $> E_{gap}$(B3LYP) $> E_{gap}$(HCTH) $> E_{gap}$(SVWN).

IV. CONCLUSIONS

In summary, we have analyzed the performance of several DFT methods in the predictions of geometries and relative energies of C_{60}, C_{70}, and C_{50}. The reliable, efficient method for the prediction of fullerene geometry is HCTH with the 3-21G basis set. The relative stability of C_{50} isomers predicted by HCTH/3-21G is similar to that by B3LYP/6-31G(d). In terms of the predictions of geometries and relative energies of C_{50}, PM3 is an efficient method to first sort out the most stable isomers, and popular DFT methods are suitable for more refined prediction of relative energies. We have also found that the SVWN/STO-3G geometry is good for B3LYP/6-31G(d) to predict relative energy and B3LYP/6-31G(d)//SVWN/STO-3G can be used as the first screening tool for the search of the most stable isomers if computing resource permits. Because HCTH/3-21G predicts similar fullerene geometry and relative stability to B3LYP/6-31G(d), the HCTH/3-21G geometry is recommended for single-point B3LYP/6-31G(d) calculations if B3LYP/6-31G(d) is not affordable for geometry optimization. However, higher-level theoretical calculations with larger basis sets should be employed to identify the most stable isomer. The convergence criterion in single-point energy calculations should be set to at least 10^{-5} for the rms error in density. Finally GGA- and LDA-based DFT methods predict smaller HOMO-LUMO gap than the hybrid DFT methods do; more exact exchange in the hybrid DFT methods generally yields larger HOMO-LUMO gap.

ACKNOWLEDGMENTS

The first author (W.Q.T.) thanks the Japan Society for the Promotion of Science for financial support. The second author (J.K.F.) acknowledges support from the Key Laboratory for Supramolecular Structure and Material of Jilin University. The third author (Y.A.W.) is grateful to the Natural Sciences and Engineering Research Council (NSERC) of Canada for financial support. The last author (Y.A.) thanks financial support from Research and Development Applying Advanced Computational Science and Technology of the Japan Science and Technology Agency (ACT-JST) and the Ministry of Education, Culture, Sports, Science and Technology (MEXT). The calculations were carried out with the Linux cluster and the KYUCC IBM computers at Kyushu.

Downloaded 08 Sep 2006 to 137.82.31.244. Redistribution subject to AIP license or copyright, see http://jcp.aip.org/jcp/copyright.jsp

[1] H. W. Kroto, J. R. Heath, S. C. O'Brien, R. F. Curl, and R. E. Smalley, Nature (London) **318**, 162 (1985).
[2] K. M. Kadish and R. S. Ruoff, *Fullerenes: Chemistry, Physics, and Technology* (Wiley-Interscience, New York, 2000).
[3] R. Taylor, *Lecture Notes on Fullerene Chemistry* (Imperial College Press, London, 1999).
[4] *Optical and Electronic Pròperties of Fullerenes and Fullerene-Based Materials*, edited by J. Shinar, Z. V. Vardeny, and Z. H. Kafafi (Dekker, New York, 2000).
[5] *Fullerene Polymers and Fullerene Polymer Composites*, edited by P. C. Eklund and A. M. Rao (Springer, Berlin, 1999).
[6] R. Sijbesma, G. Srdanov, F. Wudl, J. A. Castoro, C. Wilkins, S. H. Friedman, D. L. DeCamp, and G. L. Kenyon, J. Am. Chem. Soc. **115**, 6510 (1993).
[7] S. Bosi, T. Da Ros, G. Spalluto, and M. Prato, Eur. J. Med. Chem. **38**, 913 (2003).
[8] P. W. Fowler and D. E. Manolopoulos, *An Atlas of Fullerens* (Clarendon, Oxford, 1995).
[9] J. Cioslowski, *Electronic Structure Calculations on Fullerenes and Their Derivatives* (Oxford University Press, New York, 1995).
[10] J. K. Feng, A. Ren, W. Q. Tian, M. Ge, Z. Li, C. Sun, X. Zheng, and M. C. Zerner, Int. J. Quantum Chem. **76**, 23 (2000).
[11] Y. Tajima and K. Takeuchi, J. Org. Chem. **67**, 1696 (2002).
[12] F. Furche and R. Ahlrichs, J. Am. Chem. Soc. **124**, 3804 (2002).
[13] A. J. Stone and D. J. Wales, Chem. Phys. Lett. **128**, 501 (1986).
[14] X. Zhao, H. Goto, and Z. Slanina, Chem. Phys. **306**, 93 (2004).
[15] Z. Chen and W. Thiel, Chem. Phys. Lett. **367**, 15 (2003).
[16] K. Hedberg, L. Hedberg, D. S. Bethune, C. A. Brown, H. C. Dorn, R. D. Johnson, and M. de Vries, Science **254**, 410 (1991).
[17] K. Hedberg, L. Hedberg, M. Bühl, D. S. Bethune, C. A. Brown, and R. D. Johnson, J. Am. Chem. Soc. **119**, 5314 (1997).
[18] D. R. McKenzie, C. A. Davis, D. J. H. Cockayne, D. A. Muller, and A. M. Vassallo, Nature (London) **355**, 622 (1992).
[19] A. V. Nikolaev, T. J. S. Dennis, K. Prassides, and A. K. Soper, Chem. Phys. Lett. **223**, 143 (1994).
[20] P. M. W. Gill, B. G. Johnson, and J. A. Pople, Chem. Phys. Lett. **197**, 499 (1992).
[21] C. Adamo, M. Ernzerhof, and G. E. Scuseria, J. Chem. Phys. **112**, 2643 (2000).
[22] A. D. Boese and N. C. Handy, J. Chem. Phys. **114**, 5497 (2001).
[23] A. D. Becke, Phys. Rev. A **38**, 3098 (1988).
[24] C. Lee, W. Yang, and R. G. Parr, Phys. Rev. B **37**, 785 (1988).
[25] J. P. Perdew, K. Burke, and M. Ernzerhof, Phys. Rev. Lett. **77**, 3865 (1996); **78**, 1396(E) (1997).
[26] A. D. Becke, J. Chem. Phys. **98**, 5648 (1993).
[27] C. Adamo and V. Barone, J. Chem. Phys. **110**, 6158 (1999).
[28] C. Adamo and V. Barone, Chem. Phys. Lett. **274**, 242 (1997).
[29] A. D. Becke, J. Chem. Phys. **98**, 1372 (1993).
[30] J. C. Slater, *The Self-Consistent Field for Molecular and Solids*, Quantum Theory of Molecular and Solids Vol. 4 (McGraw-Hill, New York, 1974).
[31] S. H. Vosko, L. Wilk, and M. Nusair, Can. J. Phys. **58**, 1200 (1980).
[32] J. J. P. Stewart, J. Comput. Chem. **10**, 209 (1989).
[33] M. J. Frisch, G. W. Trucks, H. B. Schlegel *et al.*, GAUSSIAN 03, Revision C.02, Gaussian, Inc., Wallingford, CT, 2004.
[34] G. Zheng, S. Irle, and K. Morokuma, Chem. Phys. Lett. **412**, 210 (2005).
[35] W. Brockner and F. Menzel, J. Mol. Struct. **378**, 147 (1996).
[36] J. J. P. Stewart and M. B. Coolidge, J. Comput. Chem. **12**, 1157 (1991).
[37] Y. Shinohara, R. Saito, T. Kimura, G. Dresselhaus, and M. S. Dresselhaus, Chem. Phys. Lett. **227**, 365 (1994).
[38] J. K. Feng, J. Li, Z. Z. Wang, and M. C. Zerner, Int. J. Quantum Chem. **37**, 599 (1990).
[39] J. Li, J. K. Feng, and C. C. Sun, Int. J. Quantum Chem. **52**, 673 (1994).
[40] X. Zhao, J. Phys. Chem. B **109**, 5267 (2005).
[41] S. Díaz-Tendero, M. Alcamí, and F. Martín, Chem. Phys. Lett. **407**, 153 (2005).
[42] X. Lu, Z. Chen, W. Thiel, P. v. R. Schleyer, R. Huang, and L. Zheng, J. Am. Chem. Soc. **126**, 14871 (2004).
[43] G. Brinkmann and A. W. M. Dress, J. Algorithms **23**, 345 (1997).
[44] See EPAPS Document No E-JCPSA6-125-305632 for the relative energies, the averaged and maximum bond distance deviations, and the energy gap between the highest occupied molecular orbital (HOMO) and the lowest unoccupied molecular orbital (LUMO) of the first 40 most stable C_{50} isomers. This document can be reached via a direct link in the online article's HTML reference section or via the EPAPS homepage (http://www.aip.org/pubservs/epaps.html).
[45] M. A. Petrukhina, K. W. Andreini, J. Mack, and L. T. Scott, J. Org. Chem. **70**, 5713 (2005).
[46] U. Salzner, J. B. Lagowski, P. G. Pickup, and R. A. Poirier, J. Comput. Chem. **18**, 1943 (1997).
[47] R. A. King, T. D. Crawford, J. F. Stanton, and H. F. Schaefer III, J. Am. Chem. Soc. **121**, 10788 (1999).
[48] W. Q. Tian, Ph.D. thesis, University of Guelph, 2001.

Downloaded 08 Sep 2006 to 137.82.31.244. Redistribution subject to AIP license or copyright, see http://jcp.aip.org/jcp/copyright.jsp